

Synchrotron radiation microtomography for the *ex-vivo* and *in-vivo* evaluation of nanoparticle-labeled stem cell homing in muscular tissue

F.Fiori^{*}, A.Farini^{**}, A.Giuliani^{*}, A.Manescu^{*}, C.Villa^{**}, Y.Torrente^{**}

^{*}Polytechnic University of Marche, Dept. SAIFET, Physical Sciences Section,
Via Brece Bianche, 60131 Ancona, Italy

^{**}IRCCS Foundation – Polyclinic Hospital and University of Milan,
Dept. of Neurological Sciences (“Dino Ferrari” Center), Stem Cell Laboratory,
Via Francesco Sforza 35, 20122 Milan, Italy

ABSTRACT

In the perspective of clinical translation of stem cell research, the possibility to detect donor cells after transplantation and to track their fate is fundamental for a better understanding of their role in the regeneration of damaged tissues. In this article we summarize the results of *ex-vivo* and *in-vivo* X-ray computed microtomography experiments for 3D visualization of stem cells labeled with iron oxide nanoparticles and transplanted via intra-arterial infusion. We show that X-ray computed microtomography offers the possibility to detect with high definition and resolution human cells after transplantation, and opens new possibilities for experimental stem cell research.

Keywords: stem cells, nanoparticle labeling, muscular dystrophy, X-ray computed microtomography

1 INTRODUCTION

This work was carried out in the frame of a more general research program aiming to use human stem cells to repair muscle damage in Duchenne Muscular Dystrophy.

In previous works by one of the authors and coworkers [1,2] it was shown that, after intra-arterial delivery to murine dystrophic muscle, human blood-derived CD133+ cells localize under the basal lamina and express the satellite cells markers M-cadherin and Myf5, differentiating into human muscle fibers causing a significant amelioration of skeletal muscle structure.

The elucidation of the mechanisms involved in muscle homing of stem cells can aid in improving a potential therapy for muscular dystrophy based on the systemic delivery of such stem cells.

Iron oxide nanoparticle (Endorem) labeling is a promising approach to visualize stem cells *in vivo*, and thus will help the understanding of the basic processes involved in the stem cell homing and migration [3,4]. Combining nanoparticle cell labeling and X-ray computed microtomography (μ -CT) it is possible to provide detailed information on the stem cell migration in 3D, which are not attainable by traditional methods based on 2D techniques such as histology, scanning electron and fluorescence

microscopy imaging. μ -CT gives integral information about the content of iron oxide along the beam direction as well as a relative local snapshot of the nanoparticle distribution [5], with high spatial resolution images (from 10 μ m to 1 μ m) and high signal-to-noise ratio [6,7].

2 MATERIALS AND METHODS

2.1 Cell labeling and *in-vivo* transplantation

Human blood-derived CD133+ cells were isolated from mononucleated cells collected by centrifugation (Ficoll-Hypaque; Pharmacia Biotech, Uppsala, Sweden) of several buffy coats, diluted 1:2 in RPMI 1640 medium (GIBCO, Invitrogen Life Technologies), incubated with CD133-phycoerythrin (CD133PE Miltenyi Biotech, Bergisch-Gladbach, Germany), and sorted to obtain purified CD133+ cells.

Stem cells were labeled with 250 μ g/ml Fe₃O₄ nanoparticles (Endorem). Endorem has been approved for human use and is commercially available in the form of an aqueous colloid; it is a magnetic contrast agent, based on dextran-coated iron-oxide nanoparticles, with an average size of 150 nm. Labeling was performed in RPMI 1640 medium enriched with 20 ng/ml epidermal growth factor (EGF) and 10 ng/ml basic fibroblastic growth factor (bFGF) for 24 h. The mean iron concentration in a 2 ml sample containing 1 million of cells was 88.5 μ g/ml, corresponding to an average iron content of 177 pg/cell.

The labeled CD133+ cells were injected into the femoral artery of scid/mdx mice, a dystrophic animal model that allows transplantation of human cells. Different stem cell numbers (5×10^4 , 1×10^5 and 5×10^5) were considered, at different times (0, 2, 12 and 24 h) after injection.

2.2 μ -CT experimental conditions

Ex-vivo and *in-vivo* measurements were carried out at the BM05 and ID19 beamlines, respectively, of the European Synchrotron Radiation Facility (ESRF) in Grenoble – France.

For the *ex-vivo* experiment, at different times (up to 24 hours) after cell transplantation the animals were sacrificed and Tibialis Anterior (TA) biopsies ($2 \times 2 \times 2 \text{ mm}^3$) were isolated from injected legs to be studied by μ -CT [8].

In the *in-vivo* experiment, the living animals were anesthetized and their left leg were fixed in an *ad-hoc* sample holder, so that the thigh region (about 7.5 mm height in total) was exposed to the X-ray beam.

In the first case a sample-to-detector distance of 15 mm was used, and a few preliminary measurements were performed, varying the X-ray energy values between 18 and 27 keV in order to obtain optimal conditions for the X-ray absorption contrast among the different phases contained in the samples under investigation. 1000 projections were obtained from each sample over 180° , with an exposure time of 1 s per projection. A Gadox scintillator associated to a FReLoN 2048x2048 pixel CCD camera was used as a detector, with the pixel size set to $1.65 \mu\text{m}$, giving a field of view of about 3 mm. Tibialis Anterior biopsies ($2 \times 2 \times 2 \text{ mm}^3$) were isolated from injected legs and analyzed, for different numbers of initially injected cells (5×10^5 , 1×10^5 and 5×10^4), as well as different times after the injection (2, 12 and 24 h).

In the *in-vivo* the X-ray beam energy was set to 24 keV; the detection system (2048x2048 FReLoN CCD camera) and the associated optics gave a pixel size of $7.05 \mu\text{m}$, thus resulting in a field-of-view of $14.4 \times 14.4 \times 1.8 \text{ mm}^3$ ($2048 \times 2048 \times 256$ voxels); 700 projections were considered with an acquisition time of 0.2 s/projection, giving a total radiation dose on the mouse of 40 - 45 Gy. Tomograms of the thigh region taken at 0 (actually approx. 10 min.), 2, 13 and 24 hours after injection were taken, in 3 different consecutive regions-of-interest (ROI) along the direction “parallel” to the femur, for a total thickness of 5.4 mm.

3 RESULTS

3.1 *Ex-vivo* experiments

The different absorption coefficients of the materials within the samples give rise to different peaks in the grey level scale (Fig.1). In particular, the absorption coefficient of the Endorem-labeled stem cells is higher than the one of other tissues, and in the reconstructed 3D volumes the labeled cells are visualized as red spots (Fig.2). Furthermore, it is possible to use the 3D image processing to “cancel” a phase, in order to allow a more accurate observation of the spatial distribution of each phase (Fig.3).

The signal of labeled cells was clear at all concentrations greater than 5×10^4 cells. No difference in the location of stem cells was observed at different times after injection, and stem cells appear to be distributed along the vessels. The volume fraction of migrated labeled stem cells was calculated by counting their corresponding pixels, using an algorithm that automatically separates them from other tissues (Fig.4).

In order to make sure that the Endorem signal is actually associated to the labeled CD133+ stem cells, muscle biopsies from mice injected with unlabeled cells and with “naked” Endorem nanoparticles were analyzed. No detectable signal was found in muscles injected with unlabeled CD133+ cells, as well as no Endorem nanoparticles were observed within the skeletal muscle after intra-arterial injection.

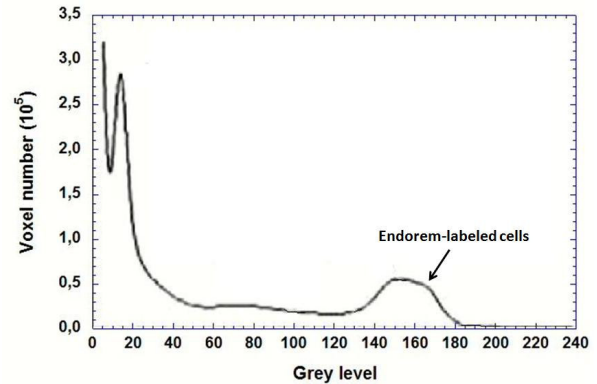


Figure 1: Grey level histogram showing the peaks corresponding to different materials in the biopsies. The peak corresponding to the Endorem-labeled cells is evidenced.

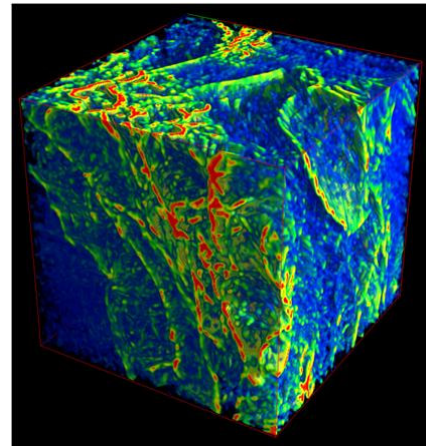


Figure 2: 3D display showing the distribution of labeled stem cells (5×10^5 injected cells, 24 h after injection; red: labeled cells, green: vessels, blue: muscular tissue).

3.2 *In-vivo* experiments

The kinetics of the migration of stem cells into the muscular tissue was followed in the living mice, after injection of 5×10^5 cells. To this end, one should notice that: i) μ -CT can reconstruct only objects that stay in place during the data acquisition, so that the signal coming from Endorem-labeled cells can only be due to cells that have actually migrated into the tissue, and not to those remained in the blood stream inside the vessels; ii) the small movements of the anesthetized animals, essentially due to

their heartbeat (~ 10 Hz), induces two oscillations of the tissue during the acquisition time of each projection (0.2 s). Therefore the beam “sees” an apparent size of the cell as big as twice the oscillation amplitude; on this basis, assuming an oscillation amplitude of 200-300 μm, a factor ~ 50 in the apparent (measured) volume fraction with respect to the real one can be estimated. Anyway, even though on a relative scale, the evaluation of the time evolution of this parameter is very important for the understanding of the migration kinetics.

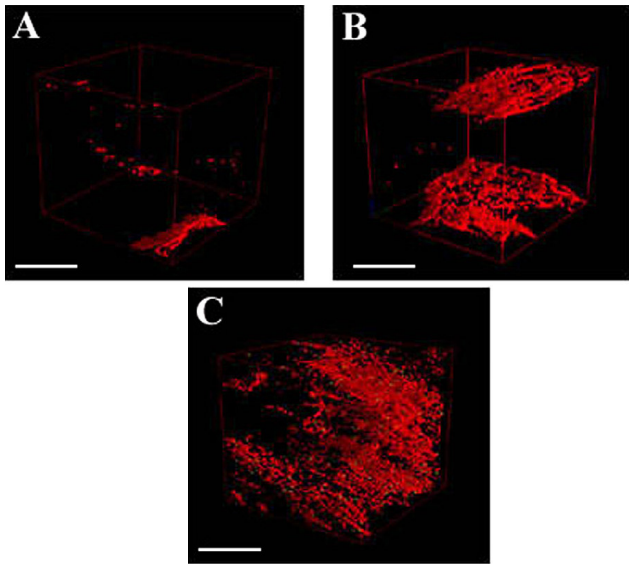


Figure 3: 3D distribution of labeled stem cells (in red) within the muscle biopsies, 12 h after injection; A) 5×10^4 , B) 1×10^5 , C) 5×10^5 injected cells (the markers correspond to 700 μm).

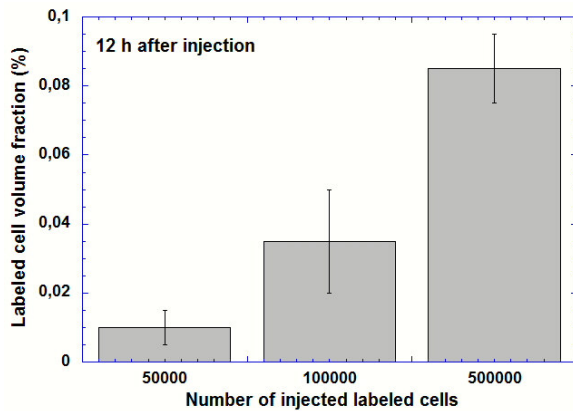


Figure 4: Volume fraction of labeled cells in the muscle biopsies, 12 h after injection.

Fig.5 shows the 3D distribution of the labeled stem cells in the investigated ROI (thigh region), for different times after injection. In order to put into evidence the stem cells

only, other tissues were eliminated by software in the image; anyway the femur bone could not be canceled, as its absorption coefficient is similar to the Endorem one and the two corresponding peaks in the grey level histogram are superimposed. Therefore, the calculation of the apparent (in the sense described above) volume fraction of the stem cells was performed excluding the thigh region where the femur is present. The result for the calculated apparent volume fraction are shown in Fig.6, in which the most important feature evidenced is that the volume fraction is saturated after 2 h. In other words, it can be concluded that the migration of the stem cells from the blood vessels to the muscular tissue happens within the first two hours from the injection.

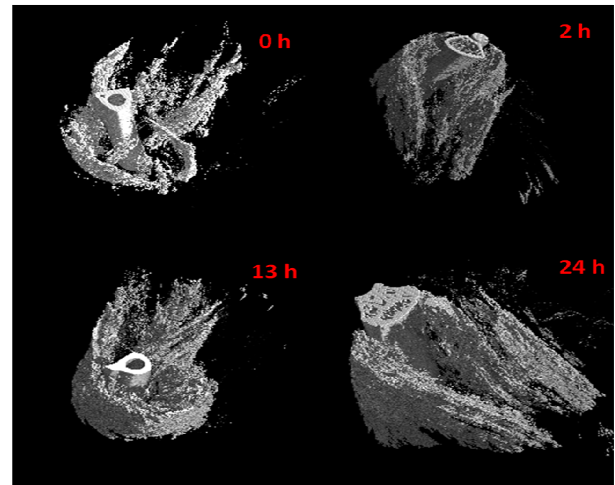


Figure 5: 3D distribution of labeled stem cells in the femur region of the living mice, at different times after injection of 5×10^5 cells.

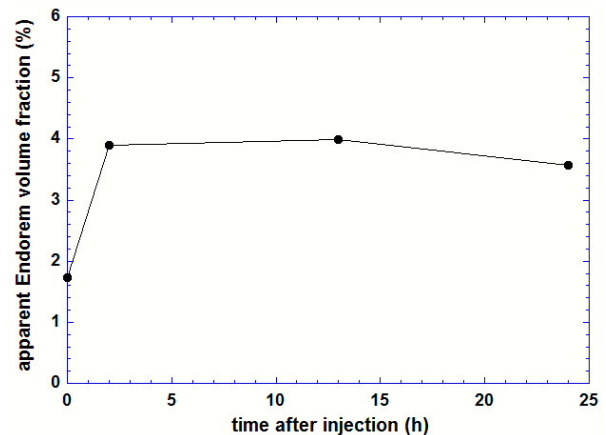


Figure 6: Time evolution of the apparent volume fraction of labeled stem cells migrated into the muscular tissue, after injection of 5×10^5 cells.

4 CONCLUSIONS

Synchrotron radiation microtomography was successfully exploited for the investigation of the homing mechanism of CD133+ human stem cells in the muscular tissue of dystrophic animal models (scid/mdx mice).

Ex-vivo experiments showed the feasibility of the technique for the visualization of Endorem-labeled stem cells, for different numbers of injected cells and at different times after injection, as well as its capability to determine the cell distribution in the tissue. It was also possible to extract quantitative parameters such as the volume fraction of migrated cells.

The kinetics of stem cell homing in the muscular tissue was studied by *in-vivo* experiments. The active blood circulation does not allow the visualization of stem cells remaining in the vessels, thus ensuring that the observed Endorem signal comes from cells migrated into the tissue only. The quantitative analysis allowed the determination, at least on a relative scale, of the volume fraction of the migrated stem cells, showing that the cell homing in the muscular tissue happens within the first two hours from the injection.

REFERENCES

- [1] Y.Torrente et al., J. Clin. Invest. 114 (2004) 182–195.
- [2] M.Gavina et al., Blood 108(8) (2006) 2857-2866.
- [3] A.K.Gupta, M.Gupta, Biomaterials 26 (2005) 3995–4021.
- [4] P.Reimer, R.Weissleder, Radiology 36 (1996) 153–163.
- [5] O.Brunkea, S.Odenbacha, C.Fritsche, I.Hilger, W.A.Kaiser, J. Magnet. Mag. Mater. 289 (2005) 428–430.
- [6] F.Peyrin, M. Salomé, P. Cloetens, A.M. Laval-Jeantet, E. Ritman, P. Ruegsegger, Technol. Health Care 6 (1998) 391.
- [7] M.Salomé, F. Peyrin, P. Cloetens, C.Odet, A.M. Laval-Jeantet, J. Baruchel, P. Spanne, Med. Phys. 26 (1999) 2194.
- [8] Y.Torrente, M.Gavina, M.Belicchi, F.Fiori, V.Komlev, N.Bresolin, F.Rustichelli, FEBS Letters 580 (2006) 5759–5764.